Laminar Boundary Layer with Hydrogen Injection Including Multicomponent Diffusion

PAUL A. LIBBY* AND MAURO PIERUCCI†
Polytechnic Institute of Brooklyn, Freeport, N. Y.

A laminar flow, which is simple from the fluid mechanical and chemical points of view, but which involves multicomponent diffusion and relatively accurate transport properties is considered. Thus a similar boundary layer with hydrogen injection and with chemical behavior idealized according to the flame sheet model is treated. On the basis of several numerical examples, it is found that the present analysis predicts a boundary-layer behavior that is significantly different from that given by analyses with simple transport; e.g., the velocity profiles with hydrogen injection resemble suction profiles because of the reduction in the $\rho\mu$ product. Accordingly, the accuracy of existing analyses involving species with a spectrum of molecular weights and employing the assumption of simple transport properties would appear doubtful.

Nomenclature

c_p = coefficient of specific heat at constant pressure
C = ratio of $\rho\mu$ products, $\rho\mu/\rho_e\mu_e$
$C_{v,\,i}/R_0$ = normalized molal specific heat of species i
$\mathfrak{D}_{ij}$ = binary diffusion coefficient
f = modified stream function
G = shear function, Cf''
h = static enthalpy
$\bar{h}$ = normalized static enthalpy, $h/h_{s,e}$
h_s = stagnation enthalpy
j_i = diffusional mass flux, $\rho_i V_i$
$\bar{j}_i$ = normalized diffusional mass flux, $j_i(2s)^{1/2}/\rho_e\mu_e u_e r^j$
L = total number of elements present
$\bar{m}$ = compressibility parameter, $u_e^2/2h_{s,\,e}$
N = total number of species present
N_h = heat-transfer coefficient, cf. Eq. (48)
p = pressure
q = energy flux
r = cylindrical radius
R = energy flux function, cf. Eq. (20)
$\bar{s}$ = transformed streamwise coordinate
T = temperature
u = streamwise velocity component
v = normal velocity component
V_i = diffusional velocity
$\dot{w}_i$ = volumetric mass rate of creation
W = molecular weight
x = streamwise coordinate
y = normal coordinate
Y_i = species mass fraction
$\tilde{Y}_j$ = element mass fraction
η = transformed normal coordinate
λ = coefficient of thermal conductivity
μ = coefficient of viscosity
μ_{ij} = number of atoms of element j in a molecule of species i
ξ = velocity ratio, f'
ρ = mass density
σ = Prandtl number, molecular diameter
ψ = stream function

Subscripts

e = value in external stream
f = value at the flame sheet
i = species, inner $0 \leq \eta \leq \eta_f$
j = element
w = value at wall or surface
0 = outer, $\eta_f \leq \eta$
1, 2, 3, 4 = O_2, H_2, H_2O, N_2, respectively

Introduction

IN the recent advances in laminar boundary-layer theory applied to chemically reacting flows, it has been customary to employ two groups of simplifying assumptions. One group pertains to the chemical behavior of the flow; in particular, one of the two limiting cases of either equilibrium chemistry or zero gas phase reaction is treated. The other group of assumptions pertains to the transport processes. It has frequently been assumed that the product of mass density and viscosity is constant, either that the Lewis number associated with the diffusion coefficient of each of the species is unity or that a single diffusion coefficient exists, and that thermal diffusion is negligible. When these assumptions are employed, great simplifications occur, and many of the solutions available from previous analyses of nonreacting boundary layers can be applied to reacting flows. The power of these assumptions has been illustrated, for example, by the work in Refs. 1–5.

The complete description of the laminar boundary layer with both groups of assumptions curtailed, i.e., with more accurate representations for the transport processes and with finite rate chemistry considered, is becoming more tractable by finite difference methods and large scale computation. However, it is the purpose of this report to present a study of a particular flow in which the description of the transport processes will be reasonably accurate but in which the chemical behavior will still be highly idealized. In particular, there will be treated the similar flow associated with the injection of hydrogen through a porous surface with a uniform, external stream of air. The static pressure will be assumed sufficiently high and the temperature conditions to be such that equilibrium chemical behavior as approximated by the flame sheet model prevails. A single product from the oxidation of the hydrogen, namely water, will be assumed. Accordingly, four species O_2, H_2, H_2O, and N_2 will exist in the boundary layer; since the molecular weights of these four may be considered in three widely different groups, namely O_2 and N_2, H_2O, and H_2, an accurate description of the diffusive behavior of the mixture does not allow a single

Received February 20, 1964; revision received June 26, 1964. This research was supported in part by the U. S. Air Force, Office of Aerospace Research, Aerospace Research Laboratories, under Contract No. AF 33(616)-7661, Project No. 7064, Task No. 7064-01, "Research on Hypersonic Flow Phenomena," and is partially supported by the Ballistic Systems Division. Andrew Boreske Jr. is the contract monitor.

* Professor of Aerospace Engineering; now Professor of Aerospace Engineering, University of California at San Diego, La Jolla, Calif. Associate Fellow Member AIAA.
† NASA Trainee. Student Member AIAA.

diffusion coefficient to be introduced, i.e., multicomponent diffusion must be considered. Thus there will not be employed the usual binary mixture approximation, which is generally applied even when more than two species are present, provided the species may be grouped into two sets of roughly constant molecular weight in each. Indeed, the principal motivation for this study resides in the treatment of a laminar boundary layer in which the diffusional fluxes are explicitly retained in the describing equations. Such a treatment would appear to have applicability to a variety of boundary layers involving complex gas mixtures, e.g., ionized gases and products of sublimation.‡ A second motivation resides in the quantitative assessment of the effect of reasonably accurate descriptions of the transport properties on the predictions of the technically interesting gross quantities such as skin friction and heat transfer. It has long been realized that flows involving gas mixtures with a spectrum of molecular weights can have significantly different behavior from that predicted by analyses based on simplified transport properties; however, there has been relatively little work devoted to a quantitative assessment of the errors involved.

The boundary layer that results from the injection of hydrogen into an air stream has been treated in the past under the assumptions of simplified chemical and transport behavior. Eckert et al.[6, 7] considered nonreacting hydrogen injection with accurate transport properties under a variety of flow conditions. Hartnett and Eckert[8] presented an analysis of the boundary layer with hydrogen injection but with constant density, with equilibrium chemistry as idealized by the flame sheet model, and with simple transport properties. Eschenroeder[9] carried out a similar analysis but for compressible flow and for the case wherein mixtures of oxygen and hydrogen are injected at the wall. Cohen et al.[2] have treated inter alia hydrogen injection under the assumptions of simple transport properties and of a chemical model based on two temperatures, one for dissociation and one for recombination. Finally, Libby and Economos[10] proposed a model for chemical reaction within a boundary layer involving contiguous regions of frozen and equilibrium flow and applied the model to the injection of oxygen-hydrogen mixtures with simple transport properties.

In the following section, the basic conservation equations involving general diffusional velocities are first transformed to similar form. The model of the chemistry of hydrogen oxidation is then discussed in order that specific boundary conditions and explicit relations for the diffusional velocities can be developed. The approximations attendant with the molecular model employed in the transport properties are then discussed. In the next section, the basic equations are put in a form convenient for numerical treatment. Finally, the results of several numerical examples are compared with those given by the usual simplified treatments and are shown to be considerably changed by consideration of multicomponent diffusion.§

Analysis

In this section, the equations for a laminar boundary layer of the similar type with four species and multicomponent diffusion are presented and put in a form suitable for numerical analysis. The basic conservation equations are discussed first. In this general discussion, the gas mixture will be assumed to consist of N species involving L elements.

‡ There have been published recently some results of large scale computations of the air system with the diffusional fluxes retained in the equations, but the main emphasis of these studies has been the computed results and not the methodology of analysis.

§ The authors are pleased to acknowledge the assistance of Leo Rute in the early stages of this study.

Conservation Equations in the Physical Variables

Consider a laminar boundary layer on a surface with a uniform external stream. Within the boundary-layer approximation, only the components of the diffusional velocities normal to the surface, i.e., in the y direction, need be considered. Accordingly, the following equations apply¶:

x-Wise Momentum

$$\rho u u_x + \rho v u_y = (\mu u_y)_y \tag{1}$$

Global Continuity

$$(\rho u r^i)_x + r^i(\rho v)_y = 0 \tag{2}$$

Species Continuity

$$\rho u(Y_i)_x + \rho v(Y_i)_y = -(j_i)_y + \dot{w}_i \qquad i = 1, 2, \ldots N \tag{3}$$

Energy

$$\rho u(h_s)_x + \rho v(h_s)_y = -(q)_y + (\mu u u_y)_y \tag{4}$$

In Eqs. (3) and (4), there appear the diffusional mass flux of species i denoted by j_i and the energy transport q, which involves inter alia j_i according to the equation

$$q = -\lambda T_y + \sum_{i=1}^{N} j_i h_i \tag{5}$$

If Eq. (5) is substituted into Eq. (4), and if there is considered the definition of h_s, namely,

$$h_s \equiv \left(\frac{u^2}{2}\right) + \sum_{i=1}^{N} Y_i h_i \tag{6}$$

then there is obtained

$$\rho u(h_s)_x + \rho v(h_s)_y = \left[\left(\frac{\lambda}{c_p}\right)\left\{(h_s)_y - \sum_{i=1}^{N} h_i\left[(Y_i)_y + \left(\frac{c_p}{\lambda}\right) j_i\right]\right\} - [\mu(\sigma^{-1} - 1)uu_y]\right]_y \tag{7}$$

It will be convenient for later developments to consider element conservation; the species creation terms are related according to the equations

$$\sum_{i=1}^{N} \frac{\mu_{ij}\dot{w}_i}{W_i} = 0 \qquad j = 1, 2, \ldots L \tag{8}$$

These suggest the introduction of element mass fractions**

$$\tilde{Y}_j \equiv \sum_{i=1}^{N} \frac{\mu_{ij} W_j Y_i}{W_i} \qquad j = 1, 2, \ldots L \tag{9}$$

The conservation equations for elements can be obtained from Eqs. (3) multiplied by $\mu_{ij}W_j/W_i$ and summed over i; there are obtained the equations

$$\rho u(\tilde{Y}_j)_x + \rho v(\tilde{Y}_j)_y = -\left(\sum_{i=1}^{N} \frac{\mu_{ij} W_j j_i}{W_i}\right)_j \qquad j = 1, \ldots L \tag{10}$$

which involve no creation terms.††

¶ These equations may be deduced from the general equations for reacting gas flows given, e.g., in Refs. 11 (pp. 514–610) and 12, provided the usual arguments concerning thin layers and normal gradients are applied.

** The concept of element mass fractions is apparently due to Zeldovitch[13] and has been widely applied in boundary-layer theory (cf., e.g., Ref. 5).

†† As will be seen below, Eqs. (10) are especially useful in the flame sheet model. It is also noted that if, and only if, a single diffusion coefficient exists so that $j_i = -D(Y_i)_y$ does the equation for element conservation take on the usual convection-diffusion form.

Transformation to Similar Form

Assume now that the boundary and initial conditions and the chemical behavior are such that similar flow exists, i.e., that all flow and gas parameters are functions of η alone where

$$\eta \equiv \rho_e u_e r^j (2\tilde{s})^{-1/2} \int_0^y \left(\frac{\rho}{\rho_e}\right) dy \tag{11}$$

In addition, introduce in the customary way a stream function:

$$\psi = (2\tilde{s})^{1/2} f(\eta) \tag{12}$$

Then Eqs. (1, 3, 7, and 10) become

$$(Cf'')' + ff'' = 0 \tag{1a}$$

$$fY_i' - (\bar{j}_i)' + (2\tilde{s}\dot{w}_i/\rho\rho_e\mu_e u_e^2 r^{2j}) = 0 \qquad i = 1, 2, \ldots N \tag{3a}$$

$$\left[\left(\frac{C}{\sigma}\right) g'\right]' + fg' - 2\tilde{m}[C(\sigma^{-1} - 1)f'f'']' - \left[\sum_{i=1}^{N} \bar{j}_i \bar{h}_i\right]' - \left[\left(\frac{C}{\sigma}\right) \sum_{i=1}^{N} \bar{h}_i Y_i'\right]' = 0 \tag{7a}$$

$$f\tilde{Y}_j' - \sum_{i=1}^{N} \frac{\mu_{ij} W_j \bar{j}_i'}{W_i} = 0 \qquad j = 1, 2, \ldots L \tag{10a}$$

where $(\ )' \equiv \partial/\partial\eta \equiv d/d\eta$ and where $\bar{j}_i \equiv (2\tilde{s})^{1/2}(j_i/\rho_e\mu_e u_e r^j) = \bar{j}_i(\eta)$.

These equations for similar flow are in rather general form and must be supplemented by statements of the boundary conditions, by descriptions of the transport properties implicit in C and σ, and by relations yielding the diffusional fluxes in the form $\bar{j}_i$. However, it is more convenient to choose a chemical system and to specialize these equations for that system before proceeding with these statements.

A Model for the Hydrogen-Air Reaction

For the purpose of the present study, it will be sufficient to consider the case of hydrogen injection into an air stream with nitrogen treated as inert, with water as the only product, and with equilibrium chemical behavior as approximated by the flame sheet model assumed to prevail. Thus $N = 4$, $L = 3$. The flame sheet model assumes that there exists a value of $\eta = \eta_f$ such that for $0 < \eta < \eta_f$ no oxygen exists in molecular form and for $\eta > \eta_f$ no hydrogen exists in molecular form; water is formed at the surface $\eta = \eta_f$ and diffuses in both directions, i.e., toward the wall and toward the external stream.

According to this model, the complete solution for the boundary-layer properties in terms of η must be considered to consist of two solutions, one for $0 \leq \eta \leq \eta_f$ and another for $\eta \geq \eta_f$. At $\eta = \eta_f$, the bulk velocities u and v, the state properties ρ and T, the species mass fractions Y_i, and the element mass fractions $\tilde{Y}_i$ must be continuous. However, the gradients of temperature and composition are related to q', $\bar{j}_i$, Y_i', and $\tilde{Y}_i'$, and these are discontinuous across the surface defined by $\eta = \eta_f$. This can be seen more clearly by integrating Eqs. (1a, 3a, 7a, and 10a) across the line $\eta = \eta_f$, i.e., from $\eta = \eta_f - \epsilon$ to $\eta = \eta_f + \epsilon$. If f and f' are continuous, then since C is continuous, Eq. (1a) yields

$$C_f f''|_{\pm} = 0 \qquad \text{or} \qquad f''|_{\pm} = 0 \tag{13a}$$

where $(\ )|_{\pm}$ implies

$$\lim_{\epsilon \to 0} (\ )|_{\eta_f - \epsilon}^{\eta_f + \epsilon}$$

On the contrary, Eq. (3a) yields, with Y_i continuous,

$$\bar{j}_i|_{\pm} = F \int_{-}^{+} \tilde{s}\dot{w}_i d\eta \tag{13b}$$

where F is a continuous function of η evaluated at η_f; now in the flame sheet model, $\dot{w}_i(\eta_f) \to \infty$, and the integral is nonzero in the limit as $\epsilon \to 0$ so that

$$\bar{j}_i|_{\pm} \neq 0$$

for i corresponding to active species, i.e., to oxygen, hydrogen, and water. Accordingly, Eq. (7a) yields

$$q'\Big|_{-}^{+} = \sum_{i=1}^{N} h_{i,f} \left[\left(\frac{\sigma}{C}\right) \bar{j}_i - Y_i'\right]\Big|_{-}^{+} \tag{13c}$$

There appears to be no a priori reason why the right-hand side of Eq. (13c) should be zero, so that discontinuities in q' at $\eta = \eta_f$ must be expected.‡‡ Finally, Eq. (10a) yields restrictions on the $\bar{j}_i$'s, namely,

$$\sum_{i=1}^{N} \left(\frac{\mu_{ij} W_j \bar{j}_i}{W_i}\right)\Big|_{-}^{+} = 0 \tag{14}$$

It will be convenient in the further development of the analysis to use the following notation for the four species:

$$O_2 \to (\ )_1 \qquad H_2 \to (\ )_2$$
$$H_2O \to (\ )_3 \qquad N_2 \to (\ )_4 \tag{15}$$

Thus, the three element mass fractions are

$$\tilde{Y}_1 \equiv Y_1 + (W_1/2W_3)Y_3 \tag{9a}$$

$$\tilde{Y}_2 \equiv Y_2 + (W_2/W_3)Y_3 \tag{9b}$$

$$\tilde{Y}_4 \equiv Y_4 \tag{9c}$$

If the distributions of the element mass fractions are found as functions of η for the two ranges of η, then the composition is completely known by virtue of the supplemental relations

$$Y_1 \equiv 0 \qquad 0 < \eta < \eta_f$$
$$Y_2 \equiv 0 \qquad \eta > \eta_f \tag{16}$$

Note that

$$\sum_{i=1,2,4} \tilde{Y}_i \equiv 1$$

so that only two element mass fractions must be considered explicitly, the third being obtained from this identity. In this study, $\tilde{Y}_4 \equiv Y_4$ will be so determined since it tends to be relatively large. Similarly $\bar{j}_4 = -(\bar{j}_1 + \bar{j}_2 + \bar{j}_3)$, so that in each region only two diffusional flux parameters must be considered explicitly. Thus, it will be sufficient to consider explicitly only the two conservation equations for the element mass fractions, i.e., Eqs. (10a), with the "jump" condition of Eq. (14).§§

In view of Eqs. (16), it is convenient to write the species mass fractions in the two regions in terms of the element mass fractions as follows:

For $0 \leq \eta \leq \eta_f$

$$Y_1 = 0 \qquad Y_2 = \tilde{Y}_2 - (2W_2/W_1)\tilde{Y}_1$$
$$Y_3 = (2W_3/W_1)\tilde{Y}_1 \qquad Y_4 = \tilde{Y}_4 = 1 - \tilde{Y}_1 - \tilde{Y}_2 \tag{17}$$

For $\eta > \eta_f$

$$Y_1 = \tilde{Y}_1 - (W_1/2W_2)\tilde{Y}_2 \qquad Y_2 = 0$$
$$Y_3 = (W_3/W_2)\tilde{Y}_2 \qquad Y_4 = \tilde{Y}_4 = 1 - \tilde{Y}_1 - \tilde{Y}_2 \tag{18}$$

‡‡ This is in contrast to the usual treatments of the flame sheet model with simplified transport properties wherein $q'|_{\pm} = 0$ because the right side is zero identically.

§§ The point of view to be taken with respect to Eq. (13b) is that the right-hand side takes on whatever value required to obtain the "jump" in $\bar{j}_i$.

Clearly, Eqs. (17) and (18) can be differentiated with respect to η to yield the derivatives Y_i', $i = 1, 2, 3, 4$ in terms of the derivatives $\tilde{Y}_i'$, $i = 1, 2$.

Corresponding to Eqs. (16) are the following relations pertinent to the diffusional mass fluxes:

$$\bar{j}_1 = 0 \qquad 0 < \eta < \eta_f$$
$$\bar{j}_2 = 0 \qquad \eta > \eta_f \tag{19}$$

With these conditions the restrictions on the $\bar{j}_i$'s at the flame sheet given by Eq. (14) become as follows:

$$(\bar{j}_i)^+ = (W_1/2W_3)[(\bar{j}_3)^- - (\bar{j}_3)^+]$$
$$(\bar{j}_2)^- = (W_2/W_3)[(\bar{j}_3)^+ - (\bar{j}_3)^-] \tag{14a}$$

Final Differential Equations

It is now convenient to anticipate the numerical analysis and thus to present the final equations for momentum, energy, and element conservation for each region in terms of first-order differential equations. In order to avoid differentiation of transport properties, it is convenient to introduce the following new variables:

$$G \equiv Cf'' \qquad \xi \equiv f'$$
$$\begin{aligned} R_i \equiv\ & (C/\sigma)g' - 2\tilde{m}C(\sigma^{-1} - 1)f'f'' - \bar{h}_2\{\bar{j}_2 + \\ & (C/\sigma)[\tilde{Y}_2' - (2W_2/W_1)\tilde{Y}_1']\} - \\ & \bar{h}_3\{\bar{j}_3 + (C/\sigma)(2W_3/W_1)\tilde{Y}_1'\} + \\ & \bar{h}_4\{\bar{j}_2 + \bar{j}_3 + (C/\sigma)(\tilde{Y}_1' + \tilde{Y}_2')\} \end{aligned} \tag{20}$$
$$\begin{aligned} R_0 \equiv\ & (C/\sigma)g' - 2\tilde{m}C(\sigma^{-1} - 1)f'f'' - \\ & \bar{h}_1\{\bar{j}_1 + (C/\sigma)[\tilde{Y}_1' - (W_1/2W_2)\tilde{Y}_2']\} - \\ & \bar{h}_3\{\bar{j}_3 + (C/\sigma)(W_3/W_2)\tilde{Y}_2'\} + \\ & \bar{h}_4\{\bar{j}_1 + \bar{j}_3 + (C/\sigma)(\tilde{Y}_1' + \tilde{Y}_2')\} \end{aligned}$$

If Eqs. (20) are substituted into Eqs. (1a) and (7a), and if Eqs. (10a) are considered in view of the model and notation employed here, the following equations are obtained:

For all η

$$G' = -\xi G/C \tag{21}$$
$$\xi' = G/C \tag{22}$$

For $0 \leq \eta \leq \eta_f$

$$R_i' = -fg' \tag{23}$$
$$\begin{aligned} g' = (\sigma/C)\{ & R_i + 2\tilde{m}\xi G(\sigma^{-1} - 1) + \\ & \bar{h}_2\{\bar{j}_2 + (C/\sigma)[\tilde{Y}_2' - (2W_2/W_1)\tilde{Y}_2']\} + \\ & \bar{h}_3\{\bar{j}_3 + (C/\sigma)(2W_3/W_1)\tilde{Y}_2'\} - \\ & h_4\{\bar{j}_2 + \bar{j}_3 + (C/\sigma)(\tilde{Y}_1' + \tilde{Y}_2')\}\} \end{aligned} \tag{24}$$

For $\eta_f \leq \eta$

$$R_0' = -fg' \tag{25}$$
$$\begin{aligned} g' = (\sigma/C)\{ & R_0 + 2\tilde{m}\xi G(\sigma^{-1} - 1) + \\ & \bar{h}_1\{\bar{j}_1 + (C/\sigma)[Y_1' - (W_1/2W_2)\tilde{Y}_2']\} + \\ & \bar{h}_3\{\bar{j}_3 + (C/\sigma)(W_3/W_2)\tilde{Y}_2'\} - \\ & \bar{h}_4\{\bar{j}_1 + \bar{j}_3 + (C/\sigma)(\tilde{Y}_1' + \tilde{Y}_2')\}\} \end{aligned} \tag{26}$$

For $0 \leq \eta \leq \eta_f$

$$\bar{j}_3' = f(2W_3/W_1)\tilde{Y}_1' \tag{27}$$
$$\bar{j}_2' = f[\tilde{Y}_2' - (2W_2/W_1)\tilde{Y}_1'] \tag{28}$$

For $\eta_f < \eta$

$$\bar{j}_1' = f[\tilde{Y}_1' - (W_1/2W_2)\tilde{Y}_2'] \tag{29}$$
$$\bar{j}_3' = f(W_3/W_2)\tilde{Y}_2' \tag{30}$$

It will be shown below that the differential quantities $\tilde{Y}_i'$ can be expressed in terms of finite quantities; thus the right-hand sides of Eqs. (23–30) involve only finite quantities, and the preceding equations are in the form suitable for integration by standard numerical techniques.

Boundary Conditions at the Wall

With the final conservation equations available consider next the boundary conditions at the wall. The conditions on f are easily specified; from Eqs. (13a) and (13b) and the transformation equations $(x, y) \rightarrow (s, \eta)$ with $f_w' = 0$, there is obtained for the bulk mass flux $(\rho v)_w$ the usual relation

$$(\rho v)_w = \rho_e u_e[\mu_e r^j/(2s)^{1/2}](-f_w) \tag{31}$$

Note from Eq. (31) the well-known distribution of mass flux at the surface required for similar flows, i.e., $(\rho v)_w \sim x^{-1/2}$ for $(-f_w)$ to be constant. Thus the boundary conditions on f are, at $\eta = 0$,

$$f = f_w = \text{const} \qquad f' = 0 \tag{32}$$

The boundary condition on g at $\eta = 0$ is here specified only indirectly; it seems most reasonable for comparison purposes to fix the wall temperature T_w; thus the wall enthalpy ratio g_w is determined once the composition at the surface is known. Note that here a heat balance at the wall is not imposed, since it is assumed that either an arbitrary coolant temperature or a cooling mechanism exists so that the prescribed T_w prevails.

It will be assumed that pure hydrogen is injected; thus the bulk velocity of water and nitrogen must vanish at $\eta = 0$. Note that according to the flame sheet model employed herein, there is no oxygen in the inner layer $0 \leq \eta \leq \eta_f$ so that no explicit relation concerning oxygen flux at the wall is required. Now by definition of the diffusional velocities there are obtained

$$v_{3w} = v_w + V_{3w} = 0 \qquad v_{4w} = v_w + V_{4w} = 0 \tag{33}$$

so that some rearrangement, using the definitions of $\bar{j}_i$ and the Eqs. (17) and (31), yields the following convenient expressions for the diffusion fluxes:

$$\bar{j}_{2,w} = (-f_w)[1 - \tilde{Y}_2 + (2W_2/W_1)\tilde{Y}_1]_w$$
$$\bar{j}_{3,w} = (-f_w)[-(2W_3/W_1)\tilde{Y}_1]_w \tag{34}$$

Equations (34) thus relate the wall values of the diffusional parameters $\bar{j}_i$ and of the concentrations $\tilde{Y}_i$.

Boundary Conditions at Infinity

The conditions to be imposed for large η are those that make the solutions compatible with the external flow. Thus, as $\eta \rightarrow \infty$,

$$f' = 1 \qquad g = 1 \qquad \tilde{Y}_1 = \tilde{Y}_{1,e}$$
$$\tilde{Y}_2 = 0 \qquad \tilde{Y}_4 = Y_{4,e} = 1 - \tilde{Y}_{1,e} \tag{35}$$

Diffusional Fluxes

In the boundary layer under consideration, the diffusional flux parameters $\bar{j}_i$ will depend on concentration gradients and on thermal gradients. In the present study, the effect of thermal diffusion will be neglected; however, at the flame sheet, severe temperature gradients will occur so that some effect of thermal diffusion may prevail even though the thermal diffusion coefficients are generally small.¶¶

Here the diffusional velocities are related explicitly to the concentration gradients by the binary diffusion coefficients.

¶¶ According to the method of solution employed here, the inclusion of this effect should not be difficult.

Accordingly, the $\bar{\jmath}_i$ parameters will depend on gradients of the concentrations of all species. The appropriate equations can be derived as follows: On each side of the flame sheet, only three species are present; thus, consider explicitly the inner region $0 \leq \eta < \eta_f$. After either Ref. 11 (p. 516) or Ref. 12 (p. 244) the diffusional velocities V_i, $i = 2, 3, 4$ are related in matrix form to $(Y_i)_y$ according to

$$V_i = \sum_j C_{ij}(Y_j)_y \tag{36}$$

in contrast to the usual Fick's law $V_i \sim (Y_i)_y$. In Eq. (36), the C_{ij} coefficients are functions of the binary diffusion coefficients, of the concentrations, and of molecular weights. Now Eq. (36) can be put in a form convenient for the present study. Some rearrangement with the use of Eqs. (17), of the definitions $\bar{\jmath}_i$, and of the explicit expressions for the C_{ij} matrix elements leads to the following equations for $0 \leq \eta \leq \eta_f$:

$$(\mu/\mathfrak{D}_{14}\rho)C^{-1}\begin{vmatrix} a_{11}' & a_{21}' \\ a_{12}' & a_{22}' \end{vmatrix}\begin{vmatrix} \bar{\jmath}_2 \\ \bar{\jmath}_3 \end{vmatrix} = \begin{vmatrix} b_{11}' & b_{21}' \\ b_{12}' & b_{22}' \end{vmatrix}\begin{vmatrix} \tilde{Y}_1' \\ \tilde{Y}_2' \end{vmatrix} \tag{37}$$

where

$$a_{11}' = \tilde{Y}_1[(2W_4\mathfrak{D}_{14}/W_1\mathfrak{D}_{23}) - (2W_2\mathfrak{D}_{14}/W_1\mathfrak{D}_{24}) - \mathfrak{D}_{14}/\mathfrak{D}_{24}] + (\mathfrak{D}_{14}/\mathfrak{D}_{24})$$

$$a_{21}' = \tilde{Y}_1[(2W_2W_4\mathfrak{D}_{14}/W_1W_3\mathfrak{D}_{23}) - (2W_2\mathfrak{D}_{14}/W_1\mathfrak{D}_{24})] + \tilde{Y}_2[(\mathfrak{D}_{14}/\mathfrak{D}_{24}) - (W_4\mathfrak{D}_{14}/W_3\mathfrak{D}_{23})]$$

$$a_{12}' = \tilde{Y}_1[(2W_3\mathfrak{D}_{14}/W_1\mathfrak{D}_{34}) - (2W_3W_4\mathfrak{D}_{14}/W_1W_2\mathfrak{D}_{23})]$$

$$a_{22}' = \tilde{Y}_1[(2W_3\mathfrak{D}_{14}/W_1\mathfrak{D}_{34}) - (\mathfrak{D}_{14}/\mathfrak{D}_{34}) - (2W_4\mathfrak{D}_{14}/W_1\mathfrak{D}_{23})] + \tilde{Y}_2[(W_4\mathfrak{D}_{14}/W_2\mathfrak{D}_{23}) - (\mathfrak{D}_{14}/\mathfrak{D}_{24})] + (\mathfrak{D}_{14}/\mathfrak{D}_{34})$$

$$b_{11}' = \tilde{Y}_2[(2W_4/W_1) - (2W_2/W_1) - 1] + (2W_2/W_1)$$

$$b_{21}' = \tilde{Y}_1[1 - (2W_4/W_1) + (2W_2/W_1)] - 1$$

$$b_{12}' = \tilde{Y}_2[(2W_3/W_1) - (2W_3W_4/W_1W_2)] - (2W_3/W_1)$$

$$b_{22}' = \tilde{Y}_1[(2W_3W_4/W_1W_2) - (2W_3/W_1)]$$

Now it is interesting to note that if $(\mu/\mathfrak{D}_{14}\rho) \equiv C \equiv 1$ and if $\mathfrak{D}_{14}/\mathfrak{D}_{ij} \equiv 1$ for all i, j, then Eqs. (37) yield

$$(W_1/2W_3)\bar{\jmath}_3 = -\tilde{Y}_1' \tag{37a}$$

$$\bar{\jmath}_2 + (W_2/W_3)\bar{\jmath}_3 = -\tilde{Y}_2' \tag{37b}$$

so that Eqs. (27) and (28) become the usual element conservation equations applicable for the simplified transport properties related to $C = 1$, $Le_i = 1$ for all i. It is also of interest to note that the multiplying factor on the left-hand side of Eq. (37) is a Schmidt number based on $\mathfrak{D}_{14}$ divided by C.

In a similar fashion, the diffusion flux parameters in the region $\eta \geq \eta_f$ are given by the equations*

$$(\mu/\rho\mathfrak{D}_{14})C^{-1}\begin{vmatrix} a_{11}'' & a_{21}'' \\ a_{12}'' & a_{22}'' \end{vmatrix}\begin{vmatrix} \bar{\jmath}_1 \\ \bar{\jmath}_3 \end{vmatrix} = \begin{vmatrix} b_{11}'' & b_{21}'' \\ b_{12}'' & b_{22}'' \end{vmatrix}\begin{vmatrix} \tilde{Y}_1' \\ \tilde{Y}_2' \end{vmatrix} \tag{38}$$

where

$$a_{11}'' = \tilde{Y}_2[(W_4\mathfrak{D}_{14}/W_2\mathfrak{D}_{13}) - (W_1/2W_2) - 1] + 1$$

$$a_{21}'' = \tilde{Y}_1[1 - (\mathfrak{D}_{14}W_4/\mathfrak{D}_{13}W_3)] + \tilde{Y}_2[(W_1W_4\mathfrak{D}_{14}/2W_2W_3\mathfrak{D}_{13}) - (W_1/2W_2)]$$

$$a_{12}'' = \tilde{Y}_2[(W_3\mathfrak{D}_{14}/W_2\mathfrak{D}_{34}) - (W_3W_4\mathfrak{D}_{14}/W_1W_2\mathfrak{D}_{31})]$$

$$a_{22}'' = \tilde{Y}_1[(W_4\mathfrak{D}_{14}/W_1\mathfrak{D}_{31}) - (\mathfrak{D}_{14}/\mathfrak{D}_{34})] + \tilde{Y}_2[(W_3\mathfrak{D}_{14}/W_2\mathfrak{D}_{34}) - (W_4\mathfrak{D}_{14}/2W_2\mathfrak{D}_{31}) - (\mathfrak{D}_{14}/\mathfrak{D}_{34})] + (\mathfrak{D}_{14}/\mathfrak{D}_{34})$$

$$b_{11}'' = \tilde{Y}_2[1 - (W_4/W_2) + (W_1/2W_2)] - 1$$

$$b_{21}'' = \tilde{Y}_1[(W_4/W_2) - 1 - (W_1/2W_2)] + W_1/2W_2$$

$$b_{12}'' = \tilde{Y}_2[(W_3W_4/W_1W_2) - (W_3/W_2)]$$

$$b_{22}'' = \tilde{Y}_1[(W_3/W_2) - (W_3W_4/W_1W_2)] - W_3/W_2$$

Again it is noted that, if $\mu/\rho\mathfrak{D}_{14} \equiv C \equiv 1$ and if $\mathfrak{D}_{14}/\mathfrak{D}_{ij} \equiv 1$ for all i and j, then Eqs. (38) give

$$\bar{\jmath}_1 + (W_1/2W_3)\bar{\jmath}_3 = -\tilde{Y}_1' \tag{38a}$$

$$(W_2/W_3)\bar{\jmath}_3 = -\tilde{Y}_2' \tag{38b}$$

so that Eqs. (29) and (30) reduce to the usual element conservation equations valid in both regions, i.e., for all η.

It is now noted, as indicated previously, that Eqs. (37) and (38) can be solved in each region for $\tilde{Y}_i'$, $i = 1, 2$ in terms of finite quantities, and thus Eqs. (23–30) can be put in the standard form for numerical integration.

Molecular Model and the Transport Properties

The final differential equations, the boundary conditions, and the diffusion flux relations presented previously must be supplemented by equations describing the transport properties of the gas mixture. For the present study, it is considered sufficient to employ a rigid-sphere model for computing the coefficients of viscosity and of thermal conductivity and the binary diffusion coefficients. More accurate molecular models would lead to temperature variations of these coefficients somewhat different from those given by the rigid sphere model but are not considered to result in essential changes. Accordingly, it is assumed herein that (cf. Ref. 11, p. 14)

$$\mu_i = 2.67(10^{-5})(W_iT)^{1/2}\sigma_i^{-2} \text{ g/cm-sec}$$

$$\lambda_i = (\tfrac{1}{4})(R_0\mu_i/W_i)[(\tfrac{4}{15})(C_{v,i}/R_0) + (\tfrac{3}{5})] \text{ cal/cm-sec°K} \tag{39}$$

$$\mathfrak{D}_{ij} = 2.63(10^{-3})[T^3(W_i + W_j)/2W_iW_j]^{1/2}p^{-1}\sigma_{ij}^{-2} \text{ cm}^2\text{/sec}$$

where σ_i is the molecular diameter in angstroms, $\sigma_{ij} \equiv (\sigma_i + \sigma_j)/2$, where T is in degrees Kelvin, and where p is in atmospheres. In the description of the coefficient of thermal conductivity, constant values of $C_{v,i}/R_0$ representative of the values for temperatures of 2000°K have been assumed according to following:

	i	$C_{v,i}/R_0$
O_2	1	9.0
H_2	2	8.2
H_2O	3	12.0
N_2	4	8 6

(40)

The following molecular diameters have been employed here:

	i	σ_i,Å	Ref. 11
O_2	1	3.541	p. 1111
H_2	2	2.915	p. 1110
H_2O	3	2.824	p. 599
N_2	4	3.749	p. 1111

(41)

As a consequence of these approximations to the molecular properties, the quotients of the binary diffusion coefficients, $\mathfrak{D}_{14}/\mathfrak{D}_{ij}$, are constants varying from roughly 0.2 to 0.7, and the ratios μ_i/μ_e, which arise in the expressions for the transport parameter C when the mixture viscosity rule is

* Note that in the outer region the binary approximation should be quite satisfactory since no H_2 is present. It has not, however, been applied here.

considered, become constants times $(T/T_e)^{1/2}$. Similarly, it is found convenient to treat the Prandtl number as a value normalized with respect to the Prandtl number in the external stream; thus the quotients λ_i/λ_e arise and become constants times $(T/T_e)^{1/2}$.

The mixture coefficients of viscosity and conductivity, i.e., μ and λ are computed according to the mixture rules, which are due to Fay[14] and which are similar to those used previously. Thus

$$\mu = \sum_{i=1}^{N} \frac{(Y_i/W_i)\,\mu_i}{\sum_{k=1}^{N}\left(\frac{Y_k}{W_k}\right)G_{ik}} \tag{42}$$

$$\lambda = \sum_{i=1}^{N} \frac{(Y_i/W_i)\,\lambda_i}{\sum_{k=1}^{N}\left(\frac{Y_k}{W_k}\right)G_{ik}} \tag{43}$$

where

$$G_{ik} = 1 \qquad i = k$$

$$= 1.2(\sigma_{ik}/\sigma_{ii})^2(2m_{ik}/m_i)^{1/2} \qquad i \neq k$$

$$m_{ik}/m_i = W_k/(W_k + W_i)$$

Enthalpy-Temperature Relations and Their Implications

It is considered sufficiently accurate for present purposes to assume a linear relation between the species enthalpies and the temperature. Thus

$$h_i = \tilde{\Delta}_i + \bar{c}_{p,i}T \tag{44}$$

where the following values of $\tilde{\Delta}_i$ and $\bar{c}_{p,i}$ have been assumed†:

	i	$\tilde{\Delta}_i$, cal/g	$\bar{c}\theta_{pi}$, cal/g-°K
O_2	1	−124	0.283
H_2	2	−1876	4.10
H_2O	3	−3562	0.656
N_2	4	−127	0.303

(45)

As a consequence of the approximation attendant with Eq. (44), the temperature can be expressed explicitly in terms of the prime dependent variables in each region. In general there is obtained in terms of the species mass fraction

$$\theta \equiv \frac{T}{T_e} = \frac{\sum_{i=1}^{N}(Y_{i,e}\bar{c}_{p,i})}{\sum_{i=1}^{N} Y_i\bar{c}_{p,i}}\left[\frac{g - \tilde{m}f'^2 - \sum_{i=1}^{N}\left(\frac{Y_i\tilde{\Delta}_i}{h_{s,e}}\right)}{1 - \tilde{m} - \sum_{i=1}^{N}\left(\frac{Y_{i,e}\Delta_i}{h_{s,e}}\right)}\right] \tag{46}$$

When Eq. (46) is applied at the wall, it provides the expression for g_w in terms of T_w and $Y_{i,w}$.

Heat Transfer to the Wall

A result of interest from the present analysis is the heat transfer to the wall given by

$$q_w \equiv (\lambda T_y)_w - \left(\sum_{i=1}^{N}\rho_i V_i h_i\right)w \tag{47}$$

Equation (47) can be rewritten in a form more convenient for the present purposes and for the variables considered here, i.e.,

$$N_h \equiv \left[\frac{q_w(2s)^{1/2}}{\rho_e\mu_e u_e r^j h_{s,e}}\right] = \left\{\left(\frac{C}{\sigma}\right)g' - \sum_{i=1}^{N}\left[\left(\frac{C}{\sigma}\right)Y_i' + \tilde{j}_i\right]\tilde{h}_i\right\}_w \tag{48}$$

† These are the same as those used in Ref. 10 provided the slightly different form of Eq. (44) is considered.

For rates of injection sufficiently high so that the flame sheet model applies, the right-hand side of Eq. (48) results in

$$N_h = R_{i,w} \tag{49}$$

For zero injection, the equations for the outer region apply at the wall, and

$$N_h = R_{0,w} \tag{49a}$$

Numerical Analysis and Results

The only difficulty associated with obtaining numerical solutions to the describing equations by standard integration techniques pertains to the two-point boundary conditions. If the integration is started at the wall, $\eta = 0$, it is necessary to estimate four quantities, e.g., f_w'', g_w', $\tilde{Y}_{i,w}$, $i = 1, 2$ such that as $\eta \to \infty$, the conditions given by Eqs. (35) are satisfied. Thus a solution vector in a fourspace is sought; there is employed here the usual trial and error technique of establishing errors, computing influence coefficients, and then computing new estimates described, e.g., in Ref. 15. However, a difficulty associated with this technique for the present problem arises because of the restrictions which pertain to $T > 0$ and $0 \leq \tilde{Y}_i \leq 1$, $i = 1, 2, 4$, and whose violation generally halt the integration.

It was found that, unless reasonably accurate estimates of the wall quantities were used, these restrictions were not respected, and the trial and error procedure failed.‡ Indeed, as will be seen below, it was not possible to find solutions for injection rates exceeding those corresponding to $-f_w \simeq 0.1$; these are generally considered relatively low, but according to the present analysis are sufficient to cause significant changes in boundary-layer properties. These difficulties may indicate "blowoff" as defined by either $G_w = 0$ or by $\tilde{Y}_{2,w} = 1$ at surprisingly low values of f_w.

The numerical analysis was carried out on a RECOMP III computer at PIBAL employing a Kutta-Runge-Gill integration routine. Values of $\tilde{Y}_{i,w}$, $i = 1, 2$, of G_w, and of $R_{i,w}$ were assumed or computed from a previous calculation. The integration was carried forward until the location of the flame sheet where $\tilde{Y}_1 = (W_1/2W_2)\tilde{Y}_2$, i.e., where $Y_2 = 0$. The set of equations valid for $\eta > \eta_f$, and the initial conditions therefor determined from the requirements of continuity of G, ξ, and g and from Eqs. (14a) were then picked up and the integration continued. When the assumed wall parameters were close to the correct, i.e., the solution values, it was found, as might be expected, that the value of θ for large η provided a sensitive indicator which could be used to obtain the final corrections. The step-size in η, used in the integration, was reduced as a solution was approached with a final value of 0.1, except in the neighborhood of the flame sheet, where values as small as 0.02 were found necessary. The integration was carried out to a value of η between 4.5 and 6 depending upon the injection rate. A solution was considered to have been obtained when the value of θ at the extreme value of η was unity within ±2%; this resulted in satisfaction of the infinity conditions on g, f', and $\tilde{Y}_i$, $i = 1, 4$ within 0.1%.

Flow Parameters and Injection Rates

Two sets of flow conditions have been assumed for the numerical examples, one being considered representative of conditions in hypersonic flight and the other in hypersonic wind tunnels; they are taken from Ref. 10 and have the values listed in Table 1.

For each set of flow conditions, a calculation was carried out for zero injection by applying the equations for the outer region throughout the layer. The solutions in this case

‡ The existence of the flame sheet appears to preclude use of iteration procedures that were employed, e.g., in Ref. 16, and that would probably eliminate the difficulties associated with the restrictions on T and $\tilde{Y}_i$.

Table 1

	M_e, approx	$\tilde{m}$	$h_{s,e}$, cal/g	T_e, °K	T_w, °K
I	11.8	0.968	4444	900	900
II	3.8	0.810	750	900	900

correspond to an air boundary layer with reasonably accurate transport properties. Three other values of $(-f_w)$ were assumed; namely, 0.03, 0.0707, 0.106. The latter two values correspond to solutions provided by Emmons and Leigh.[17] Note that there is a minimum injection rate for which the flame sheet model of chemical behavior prevails (cf. Ref. 10); the lowest positive value of $(-f_w)$ chosen here exceeded this minimum rate.

Results in Terms of Profiles

The results of the numerical analysis are summarized in Table 2 in terms of the wall values permitting integration of a solution to be started; the results are discussed below in terms of the profiles of velocity, of stagnation enthalpy, of species mass fractions, and of temperature and in terms of the variation of wall properties with injection rate. The variation of transport properties is indicated in terms of the variation with injection rate of those properties evaluated at the wall; the severe departures from the values employed in approximate calculations are thereby emphasized.

The velocity profiles for the four rates of injection considered in each set of flow conditions are shown in Figs. 1 and 2. Also shown for comparison are representative profiles for $C \equiv 1$. It will be noted immediately that the effect of injection is opposite to that expected from previous analyses based on simple transport, namely, that the thickness of the boundary layer defined in terms of a velocity ratio close to unity is decreased by injection. It will be seen in Table 2 and also shown below that this behavior is due to the severe reduction in the $\rho\mu$ product associated with the addition of hydrogen and that the shear related to Cf'' is indeed reduced by injection.

The profiles of stagnation enthalpy are shown in Figs. 3 and 4, those of the concentrations of oxygen and hydrogen in Fig. 5, those of the concentrations of water in Fig. 6, and those of the temperature ratio θ in Figs. 7 and 8. In each case there is shown for comparison purposes the corresponding profiles as given by simple transport with $-f_w = 0.106$. Again it will be noted that significant changes in wall concentrations and profiles are associated with more accurate descriptions of transport properties. Of particular interest is the shift towards the wall of the flame sheet.

Results in Terms of Wall Values

In Fig. 9 there is shown the variation with $(-f_w)$ of the wall parameters f_w'' and G_w, and of the heat transfer characterized by N_h. It will be noted immediately that, in accord with the discussion of Figs. 1 and 2, the wall shear characterized by G_w decreases with increasing $(-f_w)$, indeed at a faster rate than that given by simplified transport, while f_w'' increases rapidly. Thus the behavior of the velocity profile is accounted for by a severe reduction in C with increasing injection, a reduction that overwhelms the decrease in G. Also to be noted is the significant difference in skin friction as characterized by G_w between the predictions of analyses with $C \equiv 1$ and with accurate transport. Similar errors in heat transfer in terms of N_h are also found.

An indication of the reason for the significant alterations in boundary-layer properties as predicted by the present

Table 2 Summary of wall values

Case	$-f_w$	$\tilde{Y}_{1,w}$	$Y_{2,w}$	G_w	$R_{1,w}$
I	0	0.232	0	0.349	0.367[a]
	0.03	0.212	0.0573	0.293	0.365
	0.0707	0.214	0.182	0.209	0.269
	0.106	0.186	0.378	0.139	0.183
II	0	0.232	0	0.437	0.375[a]
	0.03	0.210	0.0507	0.341	0.671
	0.0707	0.216	0.157	0.244	0.450
	0.106	0.196	0.330	0.165	0.263

[a] Should be denoted $R_{0,w}$ since, with no injection, R_0 applies for all η.

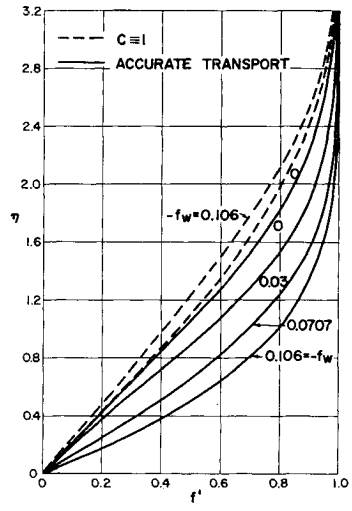

Fig. 1 Velocity profiles, $M_e \sim 11.8$.

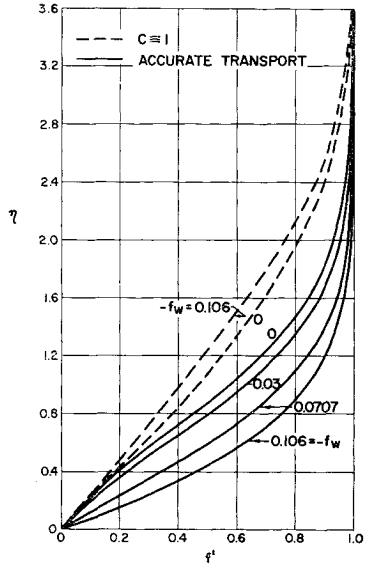

Fig. 2 Velocity profiles, $M_e \sim 3.8$.

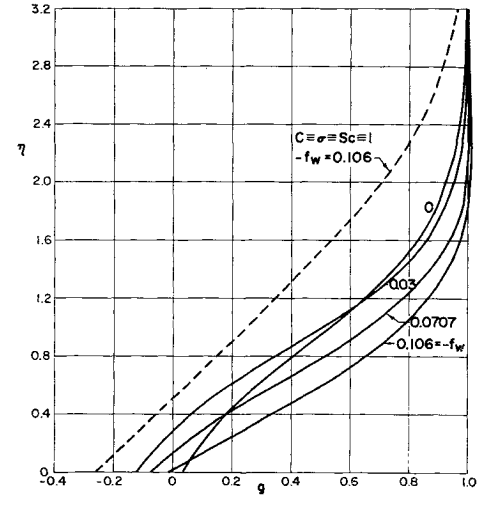

Fig. 3 Stagnation enthalpy profiles, $M_e \sim 11.8$.

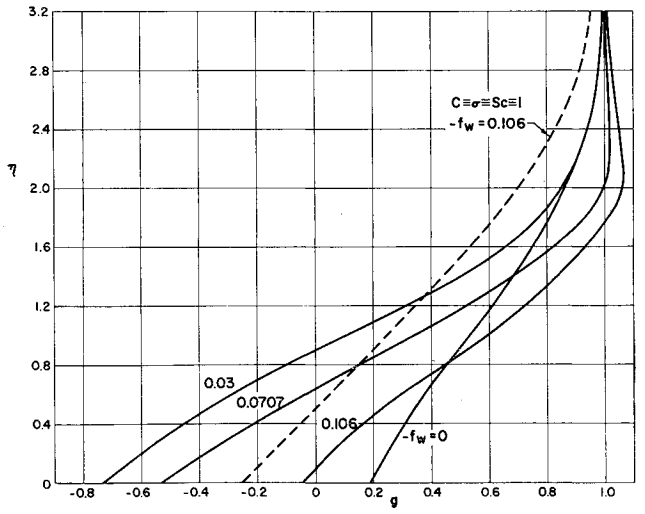

Fig. 4 Stagnation enthalpy profiles, $M_e \sim 3.8$.

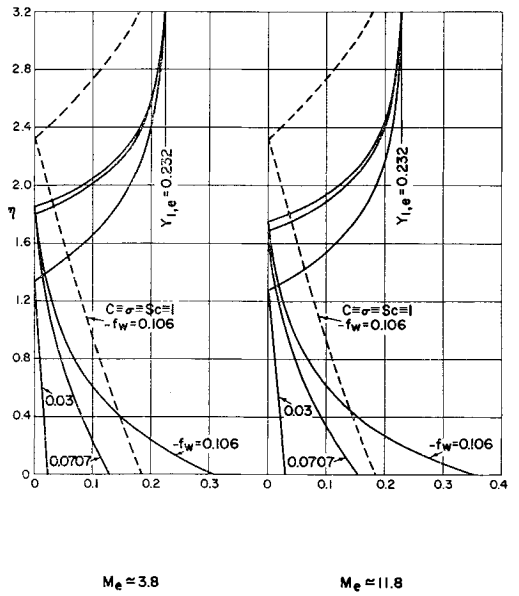

Fig. 5 Hydrogen and oxygen profiles.

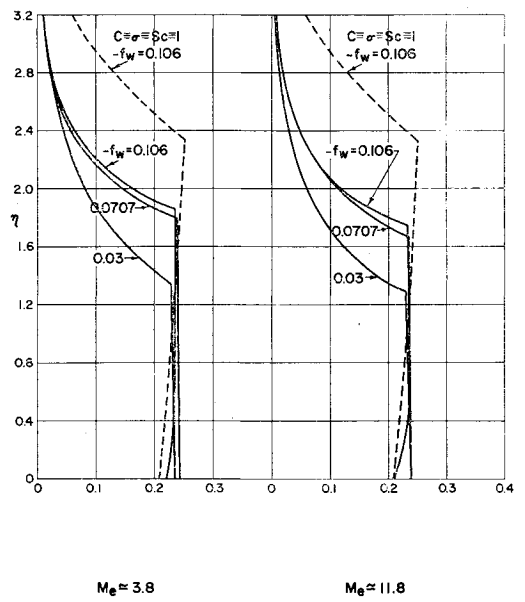

Fig. 6 Profiles of water concentration.

analysis is shown in Fig. 10, wherein the variations of C_w and of $(\mu/\rho\mathfrak{D}_{14})_w C_w^{-1}$ with $(-f_w)$ are shown. It will be noted that these parameters differ by an order of magnitude from unity, the value frequently assumed therefor. The mixture Prandtl number at the wall is found to be from 0.45 to 0.54 for $-f_w \geq 0.03$, and therefore its variation does not appear to play as important a role as the other transport parameters.

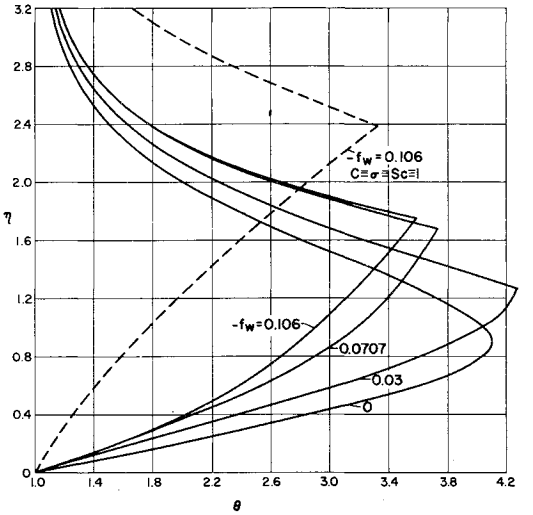

Fig. 7 Profiles of temperature ratio, $M_e \sim 11.8$.

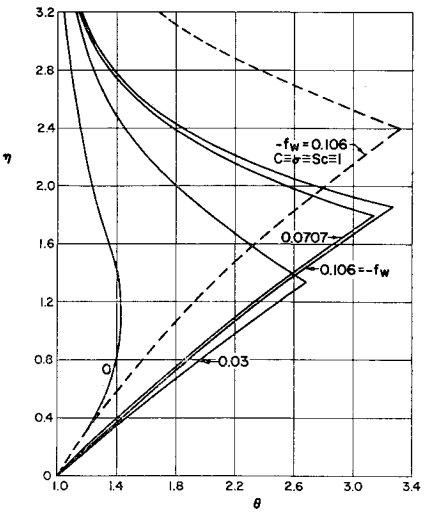

Fig. 8 Profiles of temperature ratio, $M_e \sim 3.8$.

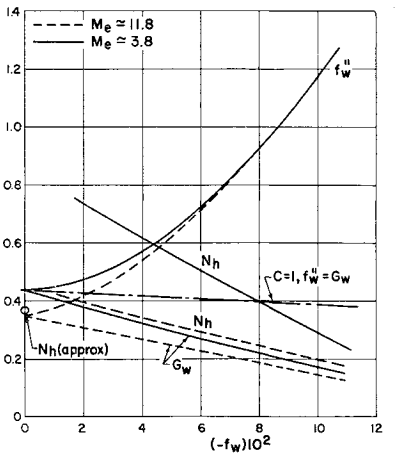

Fig. 9 Variation of flow variables at the wall with injection rate (unless indicated results are for accurate transport).

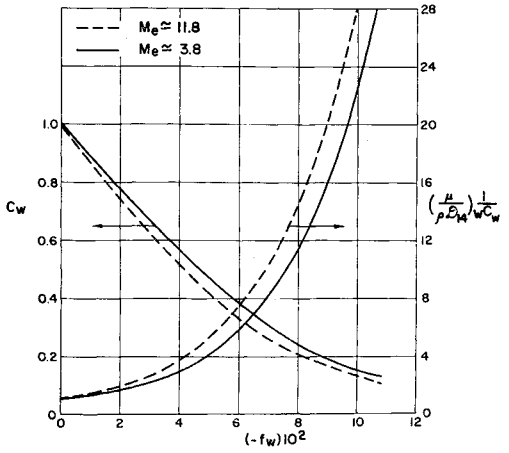

Fig. 10 Variation of transport properties at the wall with injection rate.

Concluding Remarks

An analysis has been carried out of a reacting laminar boundary layer that is relatively simple in all respects except for its transport properties. In particular, the similar flow that results from the injection of hydrogen and that is characterized by a flame sheet has been treated. Multicomponent diffusion and reasonably accurate transport properties have been considered.

Several numerical examples are presented and show significant effects of the transport properties on boundary-layer behavior. The most dramatic effect appears to be that the velocity profiles with injection resemble those usually attributed to suction; the reason for this is the severe reduction in the values of the $\rho\mu$ product due to the presence of hydrogen. Relatively large alterations in predicted skin friction and heat transfer are found.

The implication of these results seems to be that in laminar flows involving gases with a spectrum of molecular weights the predictions of analyses based on simple transport properties may be in serious error.

Appendix: Solution for the Case of Simplified Transport

For completeness and for ready reference, the solution for the flame sheet model of hydrogen injection with simplified transport properties is presented here. The analysis has been given in a somewhat different manner in Ref. 9. Make the following approximation:

$$C \cong 1 \qquad \sigma \cong 1 \qquad \mathfrak{D}_{1j}/\mathfrak{D}_{ij} \cong 1 \qquad \mu/\mathfrak{D}_{14}\rho \cong 1 \tag{A1}$$

Then the equations in the two regions $0 \leq \eta \leq \eta_f$ and $\eta > \eta_f$ become identical and are

$$f''' + ff'' = 0 \tag{A2}$$

$$f\tilde{Y}_i' + \tilde{Y}_i'' = 0 \qquad i = 1\ 2 \tag{A3}$$

$$g'' + fg' = 0 \tag{A4}$$

subject, as may be seen from Eqs. (23) and (24), to the boundary conditions at $\eta = 0$

$$\begin{aligned} f &= f_w \qquad f' = 0 \\ \tilde{Y}_1' &= (-f_w)\tilde{Y}_1 \\ \tilde{Y}_2' &= -(-f_w)(1 - \tilde{Y}_2) \\ g &= g_w \end{aligned} \tag{A5}$$

and at $\eta \to \infty$

$$= f'\ 1 \qquad \tilde{Y}_1 = \tilde{Y}_{1,e} \qquad \tilde{Y}_2 = 0 \qquad g = 1 \tag{A6}$$

The solution of Eq. (A2) subject to the boundary conditions on f in Eqs. (A5) and (A6) has been provided by Emmons and Leigh[17]§ so that $f(\eta)$ can be assumed to be given with f_w as a parameter. The solutions for $\tilde{Y}_i$, $i = 1, 2$ and for g are readily obtained in terms of f' so that the complete solution with f_w as the sole parameter is given by

$$\begin{aligned} g &= g_w + (1 - g_w)f' \\ \tilde{Y}_1 &= \{Y_{1e}/[f_w''/(-f_w) + 1]\}\{f' + [f_w''/(-f_w)]\} \\ \tilde{Y}_2 &= (1 - f')/\{[f_w''/(-f_w)] + 1\} \\ \tilde{Y}_4 &= 1 - \tilde{Y}_1 - \tilde{Y}_2 \end{aligned} \tag{A7}$$

where the wall condition specified in terms of temperature g_w is computed from Eq. (46).

References

[1] Emmons, H. W., "The film combustion of liquid fuel," Z. Angew. Math. Mech. **36**, Heft 1/2, 60–71 (January-February 1956).

[2] Cohen, C. B., Bromberg, R., and Lipkin, R. P., "Boundary layers with chemical reactions due to mass addition," Jet Propulsion **28**, 659–668 (1958).

[3] Marble, F. and Adamson, T. C., Jr., "Ignition and combustion in a laminar mixing zone," Jet Propulsion **24**, 85–94 (1954).

[4] Dooley, D. A., "Ignition in the laminar boundary layer of a heated plate," *Proceedings of the 1957 Heat Transfer and Fluid Mechanics Institute* (Stanford University Press, Stanford, Calif., 1957), pp. 321–342.

[5] Lees, L., "Convective heat transfer with mass addition and chemical reactions," *Combustion and Propulsion Third AGARD Colloquium* (Pergamon Press, New York, 1958), pp. 451–498.

[6] Eckert, E. R. C., Schneider, P. J., Hayday, A. A., and Larson, R. M., "Mass-transfer cooling of a laminar boundary layer by injection of a light-weight foreign gas," Jet Propulsion **28**, 11, 34–39 (1958).

[7] Eckert, E. R. G., Hayday, A. A., and Minkowycz, W. J., "Heat transfer, temperature recovery, and skin friction on a flat plate with hydrogen release into a laminar boundary layer," Intern. J. Heat Mass Transfer **4**, 17–29 (1961).

[8] Hartnett, J. P. and Eckert, E. R. G., "Mass transfer cooling with combustion in a laminar boundary layer," *Proceedings of the Heat Transfer and Fluid Mechanics Institute* (Stanford University Press, Stanford, Calif., 1958), pp. 65–68.

[9] Eschenroeder, A. Q., "Combustion in the boundary layer on a porous surface," J. Aerospace Sci. **27**, 901–906 (1960).

[10] Libby, P. A. and Economos, C., "A flame zone model for chemical reaction in a laminar boundary layer with application to the injection of hydrogen-oxygen mixtures," Intern. J. Heat Mass Transfer **6**, 113–128 (1963); also Polytechnic Institute of Brooklyn PIBAL Rept. 722, ARL 199 (October 1961).

[11] Hirschfelder, J. O., Curtiss, C. F., and Bird, R. B., *Molecular Theory of Gases and Liquids* (John Wiley and Sons, Inc., New York, 1954).

[12] Penner, S. S., *Chemistry Problems in Jet Propulsion* (Pergamon Press, New York, 1957).

[13] Zeldovitch, Y. B., "On the theory of combustion of initially unmixed systems," Zh. Tekh. Fiz. **19**, 1199–1210 (1944); also transl. as NACA TM 1296 (June 1950).

[14] Fay, J. A., "Hypersonic heat transfer in air laminar boundary layer," AGARD Specialists Conference, Brussels, Belgium (1962); also Avco-Everett Research Lab. Rept. AMP-71 (1962).

[15] Cohen, C. B. and Reshotko, E., "Similar solutions for the compressible laminar boundary layer with heat transfer and pressure gradient," NASA Rept. 1293 (1956).

[16] Janowitz, G. S. and Libby, P. A., "The effect of variable transport properties on a dissociated boundary layer with surface reaction," Polytechnic Institute of Brooklyn, PIBAL Rept. 804 (October 1963); also Intern. J. Heat Mass Transfer (to be published).

[17] Emmons, H. W. and Leigh, D. C., "Tabulation of the Blasius function with blowing and suction," Aeronautical Research Council Rept. 15, p. 996 (June 1953).

§ The critical parameter f_w'' as a function of f_w has been presented in terms of the present variables in Ref. 10.